Nano hydroxyapatite crystals obtained by colloidal solution

D. Meza, I.A. Figueroa, C. Flores-Morales, and M.C. Piña-Barba
Instituto de Investigaciones en Materiales, Universidad Nacional Autónoma de México, Ciudad Universitaria, Circuito exterior s/n, México. 04510 D.F. México,
mcpb@unam.mx

Recibido el 30 de mayo de 2011; aceptado el 19 de septiembre de 2011

A process for synthesising nanocrystalline hydroxyapatite powders using calcium nitrate tetrahydrated [$Ca(NO_3)_2$-$4H_2O$] and phosphorous pentoxide [P_2O_5] by colloidal solution, is presented and discussed. The powders were washed and calcinated at different temperatures and then characterised by X-ray diffraction (XRD), scanning electron microscopy (SEM) and transmission electron microscopy (TEM). The powder size was compared with the results obtained from TEM and the calculated with the Scherrer's formula.

Keywords: Hydroxyapatite; nanocrystals; X-Ray diffraction; biomaterials; colloidal solution.

En este trabajo se presenta un proceso de síntesis por solución coloidal para obtener polvos nanocristalinos de hidroxiapatita usando nitrato de calcio tetrahidratado [$Ca(NO_3)_2$-$4H_2O$] y pentóxido de fósforo [P_2O_5]. Los polvos obtenidos fueron lavados y calcinados a diferentes temperaturas para ser caracterizados empleando difracción de rayos X (DRX), microscopía electrónica de barrido (MEB) y microscopía electrónica de trasmisión (MET). El tamaño de los polvos se obtuvo comparando los resultados obtenidos por MET con los calculados por DRX usando la fórmula de Scherrer.

Descriptores: Hidroxiapatita; nanocristales; difracción de Rayos X; biomateriales; solución coloidal.

PACS: 61.05.C; 81.07.-b; 81.10.Dn

1. Introduction

In the last sixty years there have been a number of articles about the importance of hydroxyapatite (HA), a mineral that can be found in rocks and in mines, as a bone substitute biomaterial [1-10]. It has been reported in many different ways as a solid, or as a crystalline or amorphous powder, or as a coating, etc. In the last years its use has been investigated as nanocrystals (NHA) deposited on polymeric biocompatible fibres and in combination with stem cells or with plaquettes rich plasma (PRP) [11-15]; also as a coating on titanium metallic prosthesis [16-17] as well as in the drug delivery field [18-19].

HA is precisely, the main inorganic component of vertebrate bones and the main factor of the hardness and strength of bones and teeth. It forms the dental enamel, which is the hardest material known in animals due to the arrangement of the HA crystals in the teeth. The chemical formula of hydroxyapatite is: $Ca_{10-x}(PO_4)_{6-x}(OH)_{2-x}$; where $1 \geq x \geq 0$; when x = 0 is called stoichiometric HA. In the human organism the bone tissue represents 99% of calcium and 80% of phosphorus of the body reservoir.

HA is not soluble in water, just in acids because of both PO_4^{3-} as well as OH^- react with H^+:

$$Ca_{10}(PO_4)_6(OH)_2 + 14H^+ \rightarrow 10Ca^{2+} + 6H_2PO_4^- + 2H_2O$$

The stoichiometric HA is synthetically obtained in the laboratory, the size and shape can be determined by controlling the main variables from the beginning, *i.e.* reagents, temperature, reaction time, pressure and experimental process. When the HA is implanted, resorption, osteoconduction and bioactivity may occur, which makes it very valuable for medical purposes. It can be used as bone substitute in cavity filling, coating of metal implants, reinforcement in composite materials etc.

The most common method to obtain HA is the precipitation method, since large amounts of material can be collected and, most importantly, inexpensive. For certain applications, some characteristics such as bioactivity, crystal size, composition etc. must be controlled from the beginning [20-21]. Tissue Engineering also known as Regenerative Medicine uses the combination of living cells into scaffolds made out of biomaterials to improve the biological tissue functions. The objective of this work is to produce NHA for medical applications.

2. Materials and methods

The synthesis of NHA crystals was carried out by colloidal solution, the chemical reagents were: calcium nitrate tetrahydrated ($Ca(NO_3)_2$-$4H_2O$) and phosphorous pentoxide (P_2O_5). They were combined in a stoichiometric ratio, as follows:

$$\text{Ca/P} = 1.67 \qquad (1)$$

The synthesis process consisted of the following steps: a) solution, b) mixture, c) drying and d) calcination. Two different solutions were processed separately, the first one with phosphorous pentoxide using a ratio of 87.6 mL of ethanol to 4.26 g of P_2O_5 and the second with calcium nitrate tetrahydrate using a ratio of 291.95 mL of ethanol to 23.6 g of $Ca(NO_3)_2$-$4H_2O$.

Once having these two homogeneous solutions, they were mixed. This method consisted on adding the first solution to

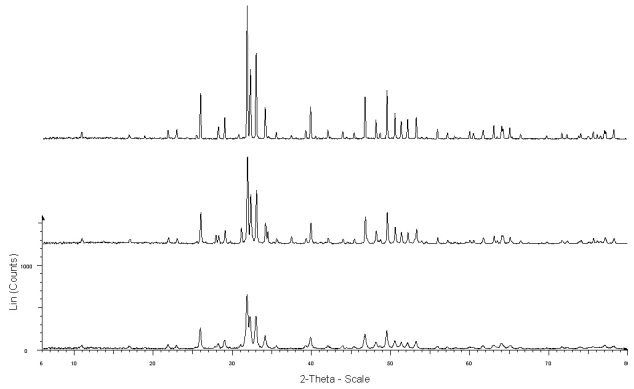

FIGURE 1. From bottom to top, the XRD patterns of samples calcined at 600, 900 and 1200°C respectively, are show. It is observed clearly that at higher temperature of calcination larger crystal sizes are obtained.

the second solution in a dropwise fashion, at a rate of 10 ml/min. The final solution was kept under magnetic stirring for an hour at room temperature. After this, the temperature was increased up to 56°C for 48 hours. The crystals obtained were ground and calcined from 600°C to 1200°C at intervals of 100°C, for 2 hours.

The powders obtained were characterized before and after calcination, by means of XRD with a Bruker AXS Diffract plus/D8 Advance diffractometer with CuKα (λ= 0.154 nm), Scanning Electron Microscopy (SEM), using a Leica Cambridge Stereoscan 440, and by Transmission Electron Microscopy (TEM) with a JEOL-JEM 1200EX. This was done in order to analyze the changes of the properties of the crystals formed, such as structure, size and morphology.

3. Results

When adding P_2O_5 to ethanol a clear solution with pH near to 0, was obtained. During this process, a white gas -like a fog- on top of the liquid was observed. A temperature raise of the solution was detected; this increment in temperature could be attributed to an exothermic reaction. When adding $Ca(NO_3)_2$-$4H_2O$ to ethanol a clear solution with pH near to 4 was obtained. In the final solution, a slow formation of white filaments was observed. These filaments had a uniform length and the number of these increased with time. After 1 hour of stirring, the mixture had a white, homogeneous and opaque appearance with higher viscosity than the initial mixture.

The mixture was dried at 56°C for 48 h, obtaining a white foam, with homogeneous porosity. The colour of the calcinated crystalline samples varied as the temperature increased, it changed from gray to bluish white. All samples had a fine grain texture similar to talc texture.

The XRD patterns of the samples calcined at 600±, 900± and 1200±C are shown in Fig. 1. The only crystalline phase present corresponds to afore mentioned stoichiometric HA; the data bank from the International for Diffraction Data (ICDD 9-432) was used in a search/match program for phase

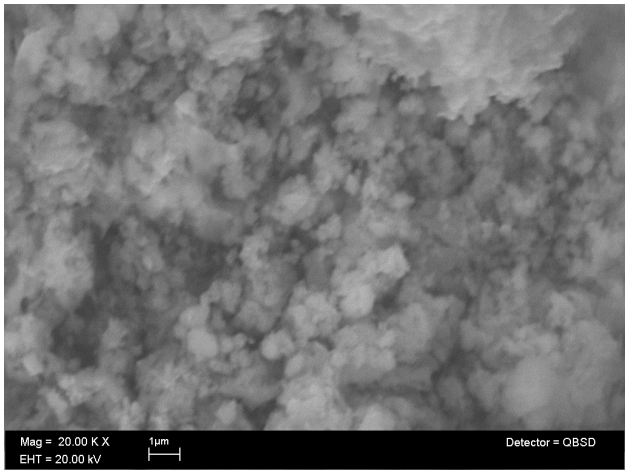

FIGURE 2. Micrograph obtained by SEM of the sample calcined at 600°C.

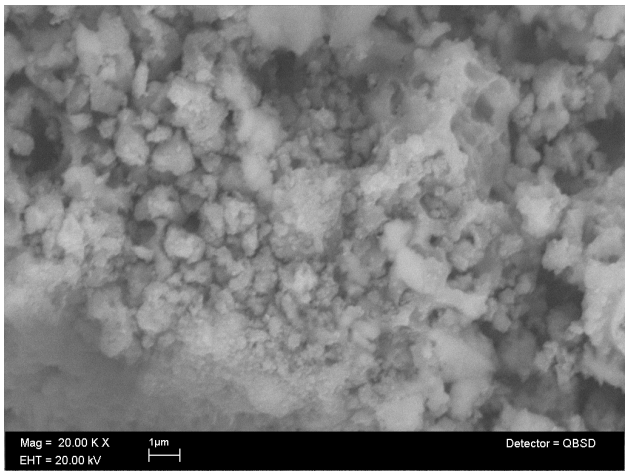

FIGURE 3. Micrograph obtained by SEM of the sample calcined at 900°C.

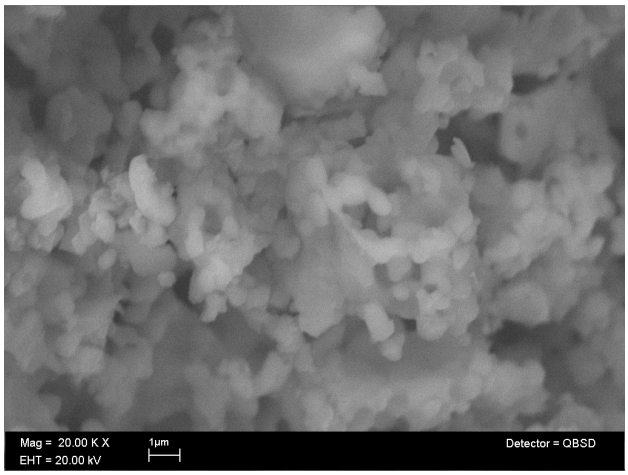

FIGURE 4. Micrograph obtained by SEM of the sample calcined at 1200°C. It is possible to observe a higher syntherization of the sample compared with the Figs. 2 and 3.

identification, the crystal size can be estimated using the full peak width at half maximum (FWHM) by using the Scherrer's formula.

$$t = (0.9)\lambda/(B\cos\theta) \tag{2}$$

where t is the average size of the particle, λ is the wavelength used, B is the FWHM and θ is the Bragg diffraction angle. With this method a particle size ranging from 25.33±4.51 nm, to 58.21 ± 2.31 nm was obtained.

For the SEM analysis, a Leica Cambridge Stereoscan 440 was used; the micrographs were obtained at 20 KX. Figures 2, 3 and 4 show the calcined powder at 600°C, 900°C y 1200°C, respectively. Similarly Figs. 5, 6 and 7 show the TEM diffraction patterns of the calcinated samples at 600°C, 900°C and 1200°C.

4. Discussion

From XRD patterns obtained, it can be observed that the width of the diffraction peaks varies inversely with calcination temperature of the sample investigated; a higher calcination temperature corresponds to a narrower width of the resulting peaks.

Using the Scherrer's formula, it is possible to make an estimate of particle size by measuring the FWHM of the highest peak of sample and comparing it with the peak of the reference crystalline sample. In this case, lanthanum hexaboride (LaB_6) was used, since it has a very high crystallinity and a diffraction pattern which resembles that of a perfect crystalline substance. In theory, the diffraction pattern of a perfect crystalline matter is composed only by Dirac deltas, which have a direct relationship with the interplanar distances of the crystal.

The width of each peak of the spectrum is composed by the contribution of the size, arrangement of the crystals and the contribution of experimental equipment, generally known as instrumental width. For crystalline samples, the width of the peaks is negligible; therefore it was assumed that the Dirac's deltas only correspond to the instrumental width. As mentioned above, in order to determine this instrumental width a crystal of LaB_6 was used. Thus, comparing the width of peaks with the instrumental width and using the Scherrer's formula, the resulting particle size is between 25.33 ± 4.51 nm and 58.21 ± 2.31 nm, as temperature increases from 600°C to 1200°C. This variation in behaviour can be observed in Fig. 8. Certainly, it is expected that the particle size will keep growing as temperature rises.

The TEM analysis showed that the particles sizes are bigger than the predicted using the Scherrer's model, specially at high calcination temperature. The powder size of the sample calcinated at 600°C agreed reasonably well with that of the theoretically calculated. However, as the temperature increases this difference became more marked. Notwithstanding the fact that the hexagonal nature of the HA crystals did play an important role in determining the crystal size by theoretical model, the difference between the experimental and

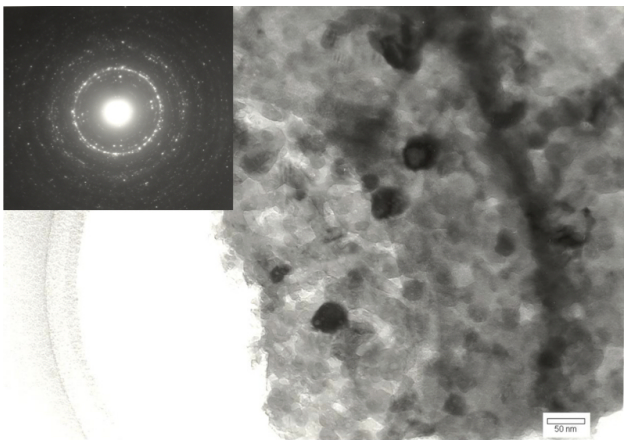

FIGURE 5. Micrograph obtained by TEM of the sample calcined at 600°C, and its diffraction pattern.

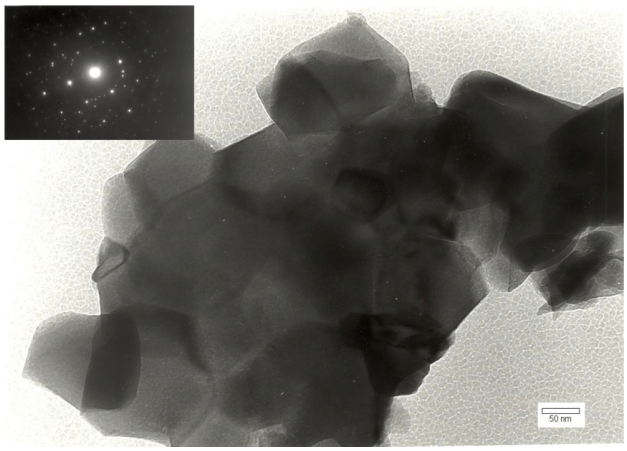

FIGURE 6. Micrograph obtained by TEM of the sample calcined at 900°C, and its diffraction pattern.

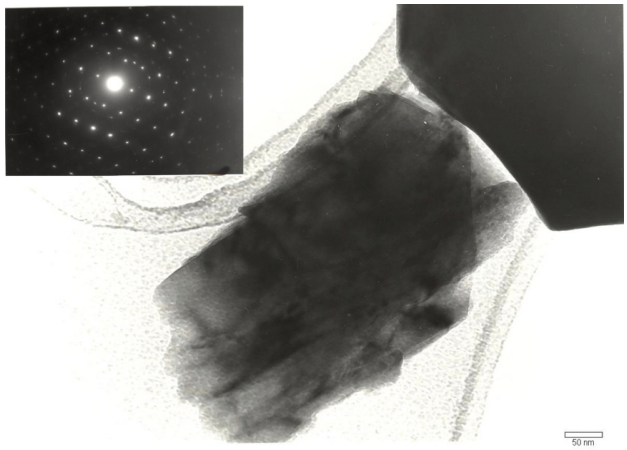

FIGURE 7. Micrograph obtained by TEM of the sample calcined at 1200°C and its diffraction pattern. It is possible to observe a higher crystalline order.

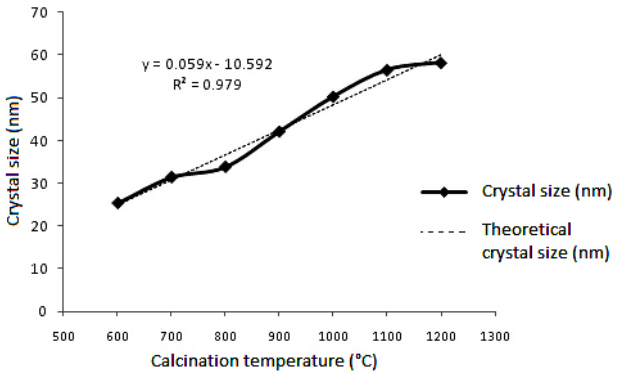

FIGURE 8. It shows dependence of crystal size with the calcined temperature calculated using Scherrer's formula and the dotted line is the linear regression of the data.

the theoretical decreased as the calcinations temperature decreases. On the other hand, this difference could be attributed to the fact that a given particle observed by TEM could be the result of the aggregation of several small particles, which the XRD analysis does differentiate. Finally, the HA produced by the aforementioned method is already being tested in biocompatibility experiments and the results will be reported elsewhere.

5. Conclusions

The method used in this work could be used to obtain hydroxyapatite nanocrystals, the sizes of the crystals obtained can ranged from 30 to 500 nm depending of the calcination temperature employed. After the synthesis, the samples had a fine grain texture similar to talc texture. Scherrer's formula can only be used for calculating the powder size as long as the widths of the peaks are much larger than the instrumental widths and, the experimental grain size is below 50 nm.

Acknowledgements

All authors would like to acknowledge DGAPA of the National Autonomous University of Mexico for the financial support trough project No. IT104011. Adriana Tejeda and Omar Novelo are also acknowledged for their technical support.

1. T.A. Kuriakose, S.N. Kalkura, M. Palanichamy, D. Arivuoli, K. Dierks, G. Bocelli, and C. Betzel, *J. Crystal Growth* **263** (2004) 517–523.
2. V.C. Guzmán, B.C. Piña, and N. Munguía, *Rev. Mex. Fis.* **51** (2005) 284-293.
3. W.C. Tsai, C.J. Liao, C.T. Wu, Y.L. Chieh, C.L. Shang, Y. Tai'Horn, W. Shing-Sheng, and L. Hwa-Chang*J. Orthopaedic Sci.* **15** (2010) 223-232.
4. S.V. Dorozhkin *J. Mat. Sc* **44** (2009) 2343-2387.
5. C. Vitale-Brovarone, F. Baino, and E. Verne *J. Mat. Sc.* **20** (2009) 643-653
6. S. Hesaraki, M. Safari, M.A. Shokrgozar, *J. Mat. Sci. Mat. In Medicine* **20** (2009) 2011-2017.
7. M.J. Sakamoto *Ceram. Soc. Japan* **118** (2010) 753-757.
8. I.M. Pelin, S.S. Maier, G.C. Chitanu, and V. Bulacovschi, *Mat. Sc. Eng. C- Mat. for Biol. App.* **29** (2009) 2188-2194.
9. K.C. Saikia, T.D. Bhattacharya, S.K. Bhuyan, D.J. Talukdar, S.P. Saikia, J.P. Indian, *J. Orthopaedics* **42** (2008) 169-172.
10. M.B. Nair, H.K. Varma, K.V. Menon, J. Sachin and A. John *Acta Biomaterialia* **5** (2009) 1742-1755.
11. M.B. Nair, H.K. Varma, and A. John, *Tissue Engineering Part A* **15** (2009) 1619-1631.
12. K. Yamamiya, K. Okuda, T. Kawase, K.I. Hata, L. Wolff, and H.J.Larry *Periodontology* **79** (2008) 811-818.
13. K. Okuda, H. Tai, K. Tanabe, H. Suzuki, T. Sato, T. Kawase, Y. Saito, L.F. Wolff, H. Yoshiex, *J. Periodontology* **76** (2005) 890-898.
14. C. Faldini, A. Moroni, and S. Giannini, *Bioceramics*, **218** (2002) 491-493.
15. A. Simunek, J. Vokurkova, D. Kopecka, M. Celko, R. Mounajjed, I. Krulichova, and Z. Skrabkova, *Clinical Oral Implants Research* **13** (2002) 75-79.
16. A. Krisanapiboon and B. Buranapanitkit, *J. Orthopaedic Sur.* **14** (2006) 315-8.
17. R. Murugan and S.J. Ramakrishna *J. Appl. Biomater, Biomech* **3** (2005) 93-7.
18. J. Liu, X. Ye, H. Wang, M. Zhu, B. Wang, and H. Yan, *Ceramics Int.* **29** (2003) 629-633.
19. E. Verron, I. Khairoun, J. Guicheux and J. Michel Bouler, *Drug Discovery Today* **15** (2010) 547-552.
20. M.R. Saeri, A. Afshara, M. Ghorbania, N. Ehsania, and C.C. Sorrell, *Materials Letters* **57** (2003) 4064–4069.
21. A. Afshara, Ghorbania, N. Ehsania, M.R. Saeria, and C.C. Sorrell, *Materials and Design* **24** (2003) 197–202.